Hall effects on peristaltic transport of a Johnson - Segalman fluid through a porous medium in a two-dimensional channel

K. SHALINI, K. ANANDA VARDHANA, AND K. RAJASEKHAR
Research Scholar, Department of Mathematics, Acharya Nagarjuna University, Guntur,
Andhra Pradesh, India.

Research Scholar, Department of Mathematics, Acharya Nagarjuna University, Guntur,
Andhra Pradesh, India.

Professor, Department of Mathematics, RVR & JC College of Engineering, Chowdavaram, Chilakuluripeta, Guntur Dist., Andhra Pradesh, India.

Abstract— In this paper, the effect of Hall on the Johnson-Segalman fluid through a porous medium in a two-dimensional channel under the assumption of long wavelength is investigated. A Closed form solutions are obtained for axial velocity and pressure gradient. The effects of various emerging parameters on the pressure gradient, time averaged volume flow rate and frictional force are discussed with the aid of graphs.

Keywords: Hall, Johnson-Segalman fluid, Hartmann number, long wavelength, peristaltic pumping, Darcy number, porous medium.

1. Introduction

Despite the fact that there are a lot of models to express non-Newtonian behavior of the fluids however in recent years, the Johnson-Segalman fluid has acquired a special class, as it includes as special cases the classical Newtonian fluid and Maxwell fluid. The Johnson-Segalman model is a viscoelastic fluid model which was developed to allow for nonaffine deformations by Johnson and Segalman (1977). Various researchers (Kolkka et al., 1988; Malkus et al., 1990; McLeish and Ball,1986) used this model to explain the happening of "spurt". The term "spurt" is worn to show the hefty increase in the volume through put for a small increase in the driving pressure gradient at a critical value of the pressure gradient that is observed in the flow of numerous non-linear fluids. Rao and Rajagopal (1999) considered three distinct flows of Johnson-Segalman fluid. Contrasting

most other fluid models, the Johnson-Segalman (JS) fluid permits for a non-monotonic relationship between the shear stress and the rate of strain in a shear flow for certain values of the material parameter. Despite the fact that the JS model offers a incredibly interesting means for elucidation "spurt", it appears more likely that the trend is because of the "stick slip" that takes place at the boundary. Peristaltic motion of a Johnson-Segalman fluid in a channel was studied by Hayat et al. (2003). Elshahed and Haroun (2005) have considered the peristaltic pumping of Johnson-Segalman fluid under effect of a magnetic field.

The basic perception regarding MHD is the magnetic field which induces the currents in conductive moving fluids which in results generates the forces on the fluid and also varies the magnetic field itself. It is well known that when any conductor comes into a magnetic field which in results creates a voltage, which is perpendicular to the current and field, this effect is known as Hall Effect. Hayat et al. (2007) have investigated the Hall effects on peristaltic flow of a Maxwell fluid in a porous medium. Effects of Hall and ion-slip currents on peristaltic transport of a couple stress fluid was analyzed by Abo-Eldahab et al. (2010). Gad (2014) has studied the effects of Hall current on peristaltic transport with compliant walls. Eldabe (2015) have studied the Hall Effect on peristaltic flow of third order fluid in a porous medium with heat and mass transfer. Hall effects on the peristaltic transport of Williamson fluid through a porous medium with heat and mass transfer was discussed by Eldabe et al. (2016). Hall effect on the peristaltic flow of a Johnson-Segalman fluid in a channel was investigated by Subba Narasimhudu (2017). Ranjitha and Subba Reddy (2018) have analyzed the radiation effects on the peristaltic flow of a Williamson fluid through a porous medium in a planar channel.

In view of these, we studied the Hall effects on the peristaltic flow of a Johnson-Segalman fluid through a porous medium in a two - dimensional channel. The flow is studied in a wave frame of reference moving with velocity of the wave under the assumptions of long-wavelength and low-Reynolds number. A Perturbation solution for small Weissenberg number is obtained for the axial velocity, axial pressure gradient and pressure rise per one wavelength. The effects of various emerging parameters on the pressure gradient and pumping characteristics are discussed with the aid of graphs.

2. Mathematical Formulation

We consider an incompressible, conducting Johnson-Segalman fluid through a porous medium confined in a two dimensional infinite symmetric channel of width 2a. We employ a rectangular coordinate system with X parallel to and Y normal to the channel walls. Moreover, we consider an infinite wave train traveling with velocity c along the channel walls. A uniform magnetic field B_0 applied in the transverse direction to the flow. Fig. 1 shows the physical model of the problem. The symmetric channel walls are defined as

$$\pm H(X,t) = \pm a \pm b \sin \left[\frac{2\pi}{\lambda} (X - ct) \right]$$
 (2.1)

Here b is the amplitudes of the waves, t is the time and λ is the wavelength.

The equations governing the flow of an incompressible fluid are

$$\operatorname{div} V = 0 \qquad \operatorname{div} \sigma + \rho f = \rho \frac{dV}{dt}$$
(2.2)

where V is the velocity field, f is the body force per unit mass, ρ is the fluid density, $\frac{d}{dt}$ is the material derivative and σ is the Cauchy stress tensor given by Johnson et al. (1977).

$$\sigma = -pI + T$$

$$(2.3)$$

$$T = 2\mu D + S$$

(2.4)

ISSN NO: 1301-2746

$$S + m \left[\frac{dS}{dt} + S(W - eD) + (W - eD)^{T} S \right] = 2\eta D$$
 (2.5)

$$D = \frac{1}{2} \left[L + L^T \right], \qquad W = \frac{1}{2} \left[L - L^T \right], \qquad L = \operatorname{grad} V$$
 (2.6)

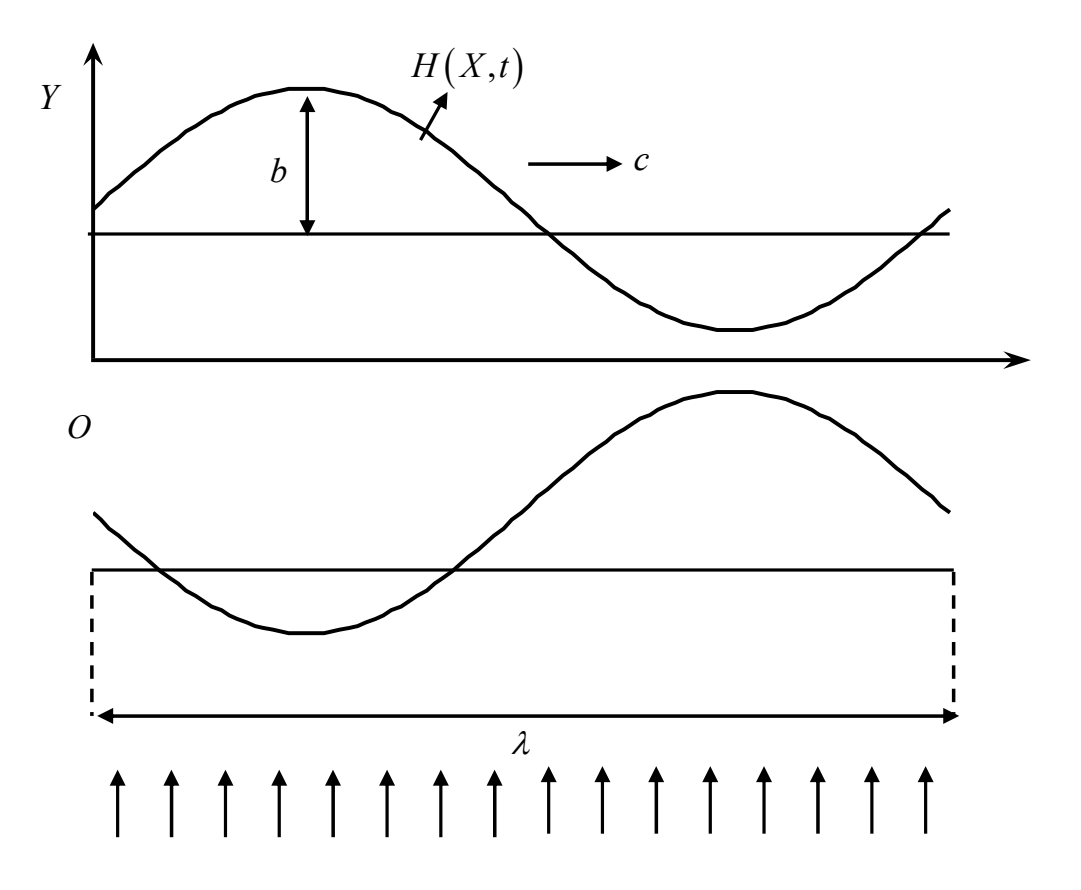


Fig. 1 The Physical Model

The equations above include the scalar pressure p, the identity tensor I, the dynamic viscosities μ and η , the relaxation time m, the slip parameter e and the respective symmetric and skew symmetric part of the velocity gradient D and W. Note that, our model reduces to the Maxwell fluid model for e=1 and $\mu=0$, and for $m=0=\mu$, it reduces to the classical Navier-Stokes fluid model.

The velocity for unsteady two-dimensional flows is defined as

$$V = \left[U(X,Y,t), V(X,Y,t), 0 \right]$$
(2.7)

In the fixed frame (X,Y) the motion is unsteady, while it becomes steady in the wave frame (x,y). The transformation from the fixed frame of reference (X,Y) to the wave frame of reference (x,y) is given by

$$x = X - ct, y = Y, u = U - c, v = V, p(x) = P(X,t)$$
 (2.8)

Here u, v and U, V are the velocity components in the wave frame and in the fixed frame, respectively.

From equations (3.2) - (3.7), we obtain, when body forces are absent, in the wave frame:

$$\frac{\partial u}{\partial x} + \frac{\partial v}{\partial y} = 0 \tag{2.9}$$

$$\rho\left(u\frac{\partial u}{\partial x} + v\frac{\partial u}{\partial y}\right) = -\frac{\partial p}{\partial x} + \mu\left(\frac{\partial^{2} u}{\partial x^{2}} + \frac{\partial^{2} u}{\partial y^{2}}\right) + \frac{\partial S_{xx}}{\partial x} + \frac{\partial S_{xy}}{\partial y} + \frac{\sigma B_{0}^{2}}{1 + m^{2}}\left(mv - \left(u + c\right)\right) - \frac{\mu}{k}\left(u + c\right)$$

(2.10)

$$\rho\left(u\frac{\partial v}{\partial x} + v\frac{\partial v}{\partial y}\right) = -\frac{\partial p}{\partial y} + \mu\left(\frac{\partial^{2} v}{\partial x^{2}} + \frac{\partial^{2} v}{\partial y^{2}}\right) + \frac{\partial S_{xy}}{\partial x} + \frac{\partial S_{yy}}{\partial y} - \frac{\sigma B_{0}^{2}}{1 + m^{2}}\left(m\left(u + c\right) + v\right) - \frac{\mu}{k}v$$

(2.11)

$$2\eta \frac{\partial u}{\partial x} = S_{xx} + m \left(u \frac{\partial}{\partial x} + v \frac{\partial}{\partial y} \right) S_{xx} - 2emS_{xx} \frac{\partial u}{\partial x} + m \left[(1 - e) \frac{\partial v}{\partial x} - (1 + e) \frac{\partial u}{\partial y} \right] S_{xy}$$

(2.12)

$$\eta \left(\frac{\partial u}{\partial y} + \frac{\partial v}{\partial x} \right) = S_{xy} + m \left(u \frac{\partial}{\partial x} + v \frac{\partial}{\partial y} \right) S_{xy} + \frac{m}{2} \left[(1 - e) \frac{\partial u}{\partial y} - (1 + e) \frac{\partial v}{\partial x} \right] S_{xx} + \frac{m}{2} \left[(1 - e) \frac{\partial v}{\partial x} - (1 + e) \frac{\partial u}{\partial y} \right] S_{yy} \tag{2.13}$$

$$2\eta \frac{\partial v}{\partial y} = S_{yy} + m \left(u \frac{\partial}{\partial x} + v \frac{\partial}{\partial y} \right) S_{yy} - 2emS_{yy} \frac{\partial v}{\partial y}$$

$$+ m \left[(1 - e) \frac{\partial u}{\partial y} - (1 + e) \frac{\partial v}{\partial x} \right] S_{xy}$$

$$(2.14)$$

Using the following non – dimensional variables

$$\overline{x} = \frac{x}{\lambda}, \quad \overline{y} = \frac{y}{a}, \quad \overline{u} = \frac{u}{c}, \quad \overline{v} = \frac{v}{c}, \quad h = \frac{H}{a}, \quad \overline{S} = \frac{a}{\mu c}S, \quad \overline{p} = \frac{a^2}{\lambda(\mu + \eta)c}p, \quad \delta = \frac{a}{\lambda},$$

$$Re = \frac{\rho ca}{\mu}, Wi = \frac{mc}{a}, \phi = \frac{b}{a}, \qquad (2.15)$$

into the equations (2.8) - (2.13), we have (after dropping the bars)

$$\frac{\partial u}{\partial x} + \frac{\partial v}{\partial y} = 0, (2.16)$$

$$\operatorname{Re} \delta \left(u \frac{\partial u}{\partial x} + v \frac{\partial u}{\partial y} \right) = -\left(\frac{\mu + \eta}{\mu} \right) \frac{\partial p}{\partial x} + \left(\delta^{2} \frac{\partial^{2} u}{\partial x^{2}} + \frac{\partial^{2} u}{\partial y^{2}} \right) + \delta \frac{\partial S_{xx}}{\partial x} + \frac{\partial S_{xy}}{\partial y} + \frac{M^{2}}{1 + m^{2}} \left(m \delta v - \left(u + 1 \right) \right) - \frac{1}{Da} \left(u + 1 \right)$$
 (2.17)

$$\operatorname{Re} \delta^{3} \left(u \frac{\partial v}{\partial x} + v \frac{\partial v}{\partial y} \right) = -\left(\frac{\mu + \eta}{\mu} \right) \frac{\partial p}{\partial y} + \delta^{2} \left(\delta^{2} \frac{\partial^{2} v}{\partial x^{2}} + \frac{\partial^{2} v}{\partial y^{2}} \right) + \delta^{2} \frac{\partial S_{xy}}{\partial x} + \delta \frac{\partial S_{yy}}{\partial y} - \frac{\delta M^{2}}{1 + m^{2}} \left(m(u+1) + \delta v \right) - \frac{\delta^{2}}{Da} v$$
(2.18)

$$\left(\frac{2\eta\delta}{\mu}\right)\frac{\partial u}{\partial x} = S_{xx} + Wi\delta\left(u\frac{\partial}{\partial x} + v\frac{\partial}{\partial y}\right)S_{xx} - 2eWi\delta S_{xx}\frac{\partial u}{\partial x}$$

$$+Wi\left(\delta^{2}\left(1-e\right)\frac{\partial v}{\partial x}-\left(1+e\right)\frac{\partial u}{\partial y}\right)S_{xy}$$
(2.19)

$$\frac{\eta}{\mu} \left(\frac{\partial u}{\partial y} + \delta^2 \frac{\partial v}{\partial x} \right) = S_{xy} + Wi\delta \left(u \frac{\partial}{\partial x} + v \frac{\partial}{\partial y} \right) S_{xy} + \frac{Wi}{2} \left[(1 - e) \frac{\partial u}{\partial y} - (1 + e) \delta^2 \frac{\partial v}{\partial x} \right] S_{xx} + \frac{Wi}{2} \left[(1 - e) \delta^2 \frac{\partial v}{\partial x} - (1 + e) \frac{\partial u}{\partial y} \right] S_{yy} \quad (2.20)$$

$$\left(\frac{2\eta\delta}{\mu}\right)\frac{\partial v}{\partial y} = S_{yy} + Wi\delta\left(u\frac{\partial}{\partial x} + v\frac{\partial}{\partial y}\right)S_{yy} - 2eWi\delta S_{yy}\frac{\partial v}{\partial y} + Wi\left((1-e)\frac{\partial u}{\partial v} - \delta^2(1+e)\frac{\partial v}{\partial x}\right)S_{xy} \tag{2.21}$$

Under lubrication approach, neglecting the terms of order δ and Re, from Equations (3.17) and (3.18), we get

$$0 = -\left(\frac{\mu + \eta}{\mu}\right) \frac{\partial p}{\partial x} + \frac{\partial^2 u}{\partial y^2} + \frac{\partial S_{xy}}{\partial y} - \left(\frac{M^2}{1 + m^2} + \frac{1}{Da}\right)(u+1)$$
 (2.22)

$$0 = -\left(\frac{\mu + \eta}{\mu}\right) \frac{\partial p}{\partial y} \qquad \Rightarrow \frac{\partial p}{\partial y} = 0 \tag{2.23}$$

where

$$S_{xx} = Wi(1+e)\frac{\partial u}{\partial y}S_{xy}$$
 (2.24)

$$\frac{\eta}{\mu} \frac{\partial u}{\partial y} = S_{xy} + \frac{Wi}{2} (1 - e) \frac{\partial u}{\partial y} S_{xx} - \frac{Wi}{2} (1 + e) \frac{\partial u}{\partial y} S_{yy}$$
 (2.25)

$$S_{yy} = -Wi(1-e)\frac{\partial u}{\partial y}S_{xy}$$
 (2.26)

$$S_{xy} + Wi^{2} \left(1 - e^{2} \right) \left(\frac{\partial u}{\partial y} \right)^{2} S_{xy} = \frac{\eta}{\mu} \frac{\partial u}{\partial y}$$
 (2.27)

From Equation (2.23), p is a function of x only. Therefore, using Equations (2.23) – (2.27), the Equation (2.22) can be rewritten as

$$\frac{dp}{dx} = \frac{\partial^2 u}{\partial y^2} + Wi^2 \alpha_1 \frac{\partial}{\partial y} \left[\left(\frac{\partial u}{\partial y} \right)^3 \right] - \frac{1}{\left(1 + \frac{\eta}{\mu} \right)} \left(\frac{M^2}{1 + m^2} + \frac{1}{Da} \right) (u + 1)$$
 (2.28)

where
$$\alpha_1 = \frac{(e^2 - 1)\eta}{(\mu + \eta)} = \frac{(e^2 - 1)}{(\gamma + 1)}, \gamma = \frac{\mu}{\eta}$$

The corresponding non - dimensional boundary conditions are

$$u = -1$$
 at $y = h = 1 + \phi \sin 2\pi x$

$$\frac{\partial u}{\partial v} = 0 \qquad \text{at} \qquad y = 0 \tag{2.29}$$

The volume flow rate in a wave frame is given by

$$q = \int_0^h u dy \tag{2.30}$$

The flux at any axial station in the laboratory frame is

$$Q(x,t) = \int_0^h (u+1)dy = q+h$$
 (2.31)

The average volume flow rate over one wave period T (= λ/c) of the peristaltic wave is defined as

$$\overline{Q} = \frac{1}{T} \int_{0}^{T} Q \, dt = q + 1 \tag{2.32}$$

3. Solution

The Equation (2.28) is non-linear and its closed form solution is not possible. Thus, we linearize this equation in terms of Wi^2 , since Wi is small for the type of flow under consideration. So we expand u, p and q as

$$u = u_0 + Wi^2 u_1 + o(Wi^4)$$

$$\frac{dp}{dx} = \frac{dp_0}{dx} + Wi^2 \frac{dp_1}{dx} + o(Wi^4)$$

$$q = q_0 + Wi^2 q_1 + o(Wi^4)$$
(3.1)

Substituting the above expressions in to the Equation (3.28) and in to the boundary conditions (3.29), we obtain

3.1 Equations of order Wi^0

$$\frac{dp_0}{dx} = \frac{\partial^2 u_0}{\partial y^2} - \frac{\gamma}{\left(1 + \gamma\right)} \left(\frac{M^2}{1 + m^2} + \frac{1}{Da}\right) \left(u_0 + 1\right) \tag{3.2}$$

The corresponding boundary conditions are

$$u_0 = -1$$
 at $y = h$ (3.3)

$$\frac{\partial u_0}{\partial y} = 0 \quad \text{at} \quad y = 0 \tag{3.4}$$

3.2 Equations of order Wi^2

$$\frac{dp_1}{dx} = \frac{\partial^2 u_1}{\partial y^2} + \alpha_1 \frac{\partial}{\partial y} \left[\left(\frac{\partial u_0}{\partial y} \right)^3 \right] - \frac{\gamma}{\left(1 + \gamma \right)} \left(\frac{M^2}{1 + m^2} + \frac{1}{Da} \right) u_1 \tag{3.5}$$

The corresponding boundary conditions are

$$u_1 = 0 \qquad \text{at} \qquad y = h \tag{3.6}$$

$$\frac{\partial u_1}{\partial y} = 0 \qquad \text{at} \qquad y = 0 \tag{3.7}$$

3.3 Solution of order Wi⁰

Solving the Equation (3.2) by using the boundary conditions (3.3) and (3.4), we get

$$u_0 = \frac{1}{\alpha^2} \frac{dp_0}{dx} \left[\frac{\cosh \alpha y}{\cosh \alpha h} - 1 \right] - 1 \tag{3.8}$$

where
$$\alpha^2 = \frac{\gamma}{(1+\gamma)} \left(\frac{M^2}{1+m^2} + \frac{1}{Da} \right)$$
.

and the volume flow rate q_0 is given by

$$q_0 = \int_0^h u_0 dy = \frac{1}{\alpha^3} \frac{dp_0}{dx} \left[\frac{\left(\sinh \alpha h - \alpha h \cosh \alpha h\right)}{\cosh \alpha h} \right] - h \tag{3.9}$$

From Equation (3.9), we obtain

$$\frac{dp_0}{dx} = \frac{\alpha^3 (q_0 + h)\cosh \alpha h}{\sinh \alpha h - \alpha h \cosh \alpha h}$$
(3.10)

3.4 Solution of order Wi^2

Solving the Equation (3.5) by using the boundary conditions (3.6) and (3.7), we get

$$u_{1} = \frac{1}{\alpha^{2}} \frac{dp_{1}}{dx} \left(\frac{\cosh \alpha y}{\cosh \alpha h} - 1 \right) + \frac{3\alpha_{1}}{2\alpha^{2}} \left(\frac{dp_{0}}{dx} \right)^{3} \left(\frac{\cos h\alpha y}{\cosh^{4} \alpha h} \right) \left[\frac{\cosh 3\alpha h}{16\alpha^{2}} - \frac{h \sinh \alpha h}{4\alpha} \right]$$

$$- \frac{3\alpha_{1}}{2\alpha^{2}} \left(\frac{dp_{0}}{dx} \right)^{3} \left(\frac{1}{\cosh^{3} \alpha h} \right) \left[\frac{\cosh 3\alpha y}{16\alpha^{2}} - \frac{y \sinh \alpha y}{4\alpha} \right]$$

$$(3.11)$$

and the volume flow rate q_1 is given by

$$q_{1} = \frac{1}{\alpha^{3}} \frac{dp_{1}}{dx} \left(\frac{\sinh \alpha h - \alpha h \cosh \alpha h}{\cosh \alpha h} \right) + \frac{3\alpha_{1}}{2\alpha^{4}} \left(\frac{A}{\cosh^{3} \alpha h} \right) \left[\frac{\alpha^{3} (q_{0} + h) \cosh \alpha h}{(\sinh \alpha h - \alpha h \cosh \alpha h)} \right]^{3}$$
(3.12)

where

$$A = \frac{\tanh \alpha h \cosh 3\alpha h}{16\alpha} - \frac{h \tanh \alpha h \sinh \alpha h}{4} - \frac{\sinh 3\alpha h}{48\alpha} + \frac{h \cosh \alpha h}{4} - \frac{\sinh \alpha h}{4\alpha}$$

From Equation (3.12), we obtain

$$\frac{dp_1}{dx} = \frac{\alpha^3 \cosh \alpha h q_1}{\sinh \alpha h - \alpha h \cosh \alpha h} - \frac{3\alpha_1 \alpha^8 A}{2} \left[\frac{(q_0 + h)^3 \cosh \alpha h}{(\sinh \alpha h - \alpha h \cosh \alpha h)^4} \right]$$
(3.13)

Substituting Equations (3.10) and (3.13) into the second equation of (3.1) and neglecting terms greater than $O(W_i^2)$, we get

$$\frac{dp}{dx} = \frac{\alpha^3 (q+h)\cosh \alpha h}{\sinh \alpha h - \alpha h \cosh \alpha h} - \frac{3\alpha_1 A \alpha^8}{2} W i^2 \left[\frac{(q+h)^3 \cosh \alpha h}{\left(\sinh \alpha h - \alpha h \cosh \alpha h\right)^4} \right]$$
(3.14)

The dimensionless pressure rise per one wavelength in the wave frame is given by

$$\Delta p = \int_0^{2\pi} \frac{dp}{dx} dx \tag{3.15}$$

where $h = 1 + \phi \sin 2\pi x$.

Note that, as $Da \to \infty$ our results coincide with the results of Subba Narasimhudu (2017). **4. Discussion of the results**

Fig. 2 illustrates the variation of the axial pressure gradient $\frac{dp}{dx}$ with Wi for $\gamma = 1$, e = 0.5, m = 0.3, M = 1, Da = 0.1, $\phi = 0.6$ and $\overline{Q} = -1$. It is found that, the axial pressure gradient $\frac{dp}{dx}$ decreases with increasing Weissenberg number Wi

The variation of the axial pressure gradient $\frac{dp}{dx}$ with γ for e=0.5, Wi=0.02, m=0.3, M=1, Da=0.1, $\phi=0.6$ and $\overline{Q}=-1$. $\overline{Q}=-1$ is illustrated in Fig. 3. It is observed that, the axial pressure gradient $\frac{dp}{dx}$ decreases with increasing γ .

Fig. 4 shows the variation of the axial pressure gradient $\frac{dp}{dx}$ with e for $\gamma = 1$, Wi = 0.02, m = 0.3, M = 1, Da = 0.1, $\phi = 0.6$ and $\overline{Q} = -1$. It is noticed that, the axial pressure gradient $\frac{dp}{dx}$ increases with increasing slip parameter e.

The variation of the axial pressure gradient $\frac{dp}{dx}$ with m for $\gamma=1, Wi=0.02$, e=0.5, M=1, Da=0.1, $\phi=0.6$ and $\overline{Q}=-1$ is shown in Fig. 5. It is observed that, the axial pressure gradient $\frac{dp}{dx}$ decreases with increasing Hall parameter m.

Fig. 6 illustrates the variation of the axial pressure gradient $\frac{dp}{dx}$ with Da for $\gamma=1, Wi=0.02$, e=0.5, m=0.3, M=1, $\phi=0.6$ and $\overline{Q}=-1$. It is found that, the axial pressure gradient $\frac{dp}{dx}$ increases with an increase in Darcy number Da.

The variation of the axial pressure gradient $\frac{dp}{dx}$ with M for $\gamma=1, Wi=0.02$, e=0.5, m=0.3, Da=0.1, $\phi=0.6$ and $\overline{Q}=-1$ is illustrated in Fig. 7. It is noticed that, the axial pressure gradient $\frac{dp}{dx}$ increases with increasing Hartmann number M.

Fig. 8 depicts the variation of the axial pressure gradient $\frac{dp}{dx}$ with ϕ for $\gamma=1$, Wi=0.02, e=0.5, m=0.3, M=1, Da=0.1 and $\overline{Q}=-1$. It is found that, the axial pressure gradient $\frac{dp}{dx}$ increases with increasing amplitude ratio ϕ .

The variation of the pressure rise Δp with \overline{Q} for different values of Wi with $\gamma=1,\ e=0.5,\ m=0.3,\ M=1, Da=0.1$ and $\phi=0.6$ is depicted in Fig. 9. It is observed that, in the pumping region $(\Delta p>0)$, the \overline{Q} decreases with increasing

weissenberg number Wi and it increases in both the free-pumping $(\Delta p = 0)$ and copumping $(\Delta p < 0)$ regions with increasing Wi.

Fig. 10 shows the variation of the pressure rise Δp with \overline{Q} for different values of γ with e=0.5, Wi=0.1, m=0.3, M=1, Da=0.1 and $\phi=0.6$. It is noticed that, in the pumping region, the \overline{Q} increases with increasing γ and it decreases in both the free-pumping and co-pumping regions with increasing γ .

The variation of the pressure rise Δp with \overline{Q} for different values of e with $\gamma=1$, Wi=0.1, m=0.3, M=1, Da=0.1 and $\phi=0.6$ is shown in Fig. 11. It is observed that, in the pumping region $(\Delta p>0)$ and pre-pumping $(\Delta p=0)$ region, the \overline{Q} increases with increasing e, while it decreases in the co-pumping $(\Delta p<0)$ region with increasing e for the chosen $\Delta p(<0)$.

Fig. 12 illustrates the variation of the pressure rise Δp with \overline{Q} for different values of m with $\gamma=1, e=0.5$, Wi=0.1, M=1, Da=0.1 and $\phi=0.6$. It is found that, in the pumping region, the \overline{Q} decreases with increasing m, while it increases in both the free-pumping and co-pumping regions with increasing m.

The variation of the pressure rise Δp with \overline{Q} for different values of Da with $\gamma=1, e=0.5$, Wi=0.1, m=0.3, Da=0.1 and $\phi=0.6$ is shown in Fig. 13. It is noticed that, in the pumping region, the \overline{Q} decreases with increasing Da, while it increases in both the free-pumping and co-pumping regions with increasing Da.

Fig. 14 depicts the variation of the pressure rise Δp with \overline{Q} for different values of M with $\gamma=1, e=0.5$, Wi=0.1, m=0.3, Da=0.1 and $\phi=0.6$. It is observed that, in the pumping region, the \overline{Q} increases with increasing M, while it decreases in both the free-pumping and co-pumping regions with increasing M.

The variation of the pressure rise Δp with \overline{Q} for different values of ϕ with $\gamma = 1, e = 0.5$, Wi = 0.1, m = 0.3, M = 1, Da = 0.1 and $\phi = 0.6$ is depicted in Fig. 15.

It is found that, in the pumping region $(\Delta p > 0)$ and pre-pumping $(\Delta p = 0)$ region, the \overline{Q} increases with increasing ϕ while it decreases in the co-pumping $(\Delta p < 0)$ region with increasing ϕ for the chosen value $\Delta p (< 0)$.

5. Conclusions

In this chapter, we studied effect of hall on the peristaltic transport of a Johnson-Segalman fluid through a porous medium in a two - dimensional channel under the assumptions of long-wavelength. Perturbation solution for small Weissenberg number is obtained for the axial velocity, axial pressure gradient and pressure rise per one wavelength. It is found that the pressure gradient $\frac{dp}{dx}$ decreases with increasing Wi, Da or m, whereas it increases with increasing γ, e, M or ϕ . In the pumping region, the time averaged flux \overline{Q} decreases with increasing Wi, Da or m, whereas it increases with increasing γ, e, M or ϕ . The friction force F first increases and then decreases with increasing Wi.

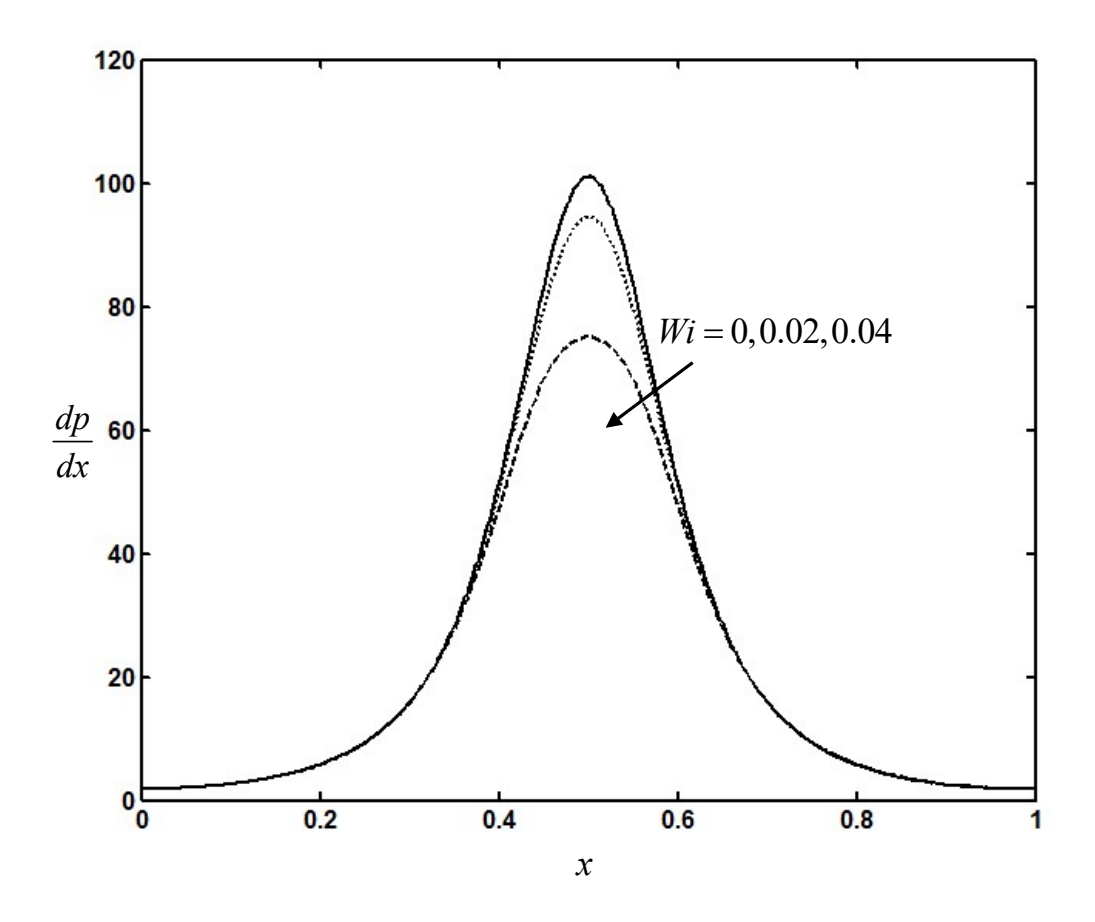


Fig. 2 The variation of the axial pressure gradient $\frac{dp}{dx}$ with Wi for $\gamma = 1$, e = 0.5, m = 0.3, Da = 0.1, M = 1, $\phi = 0.6$ and $\overline{Q} = -1$.

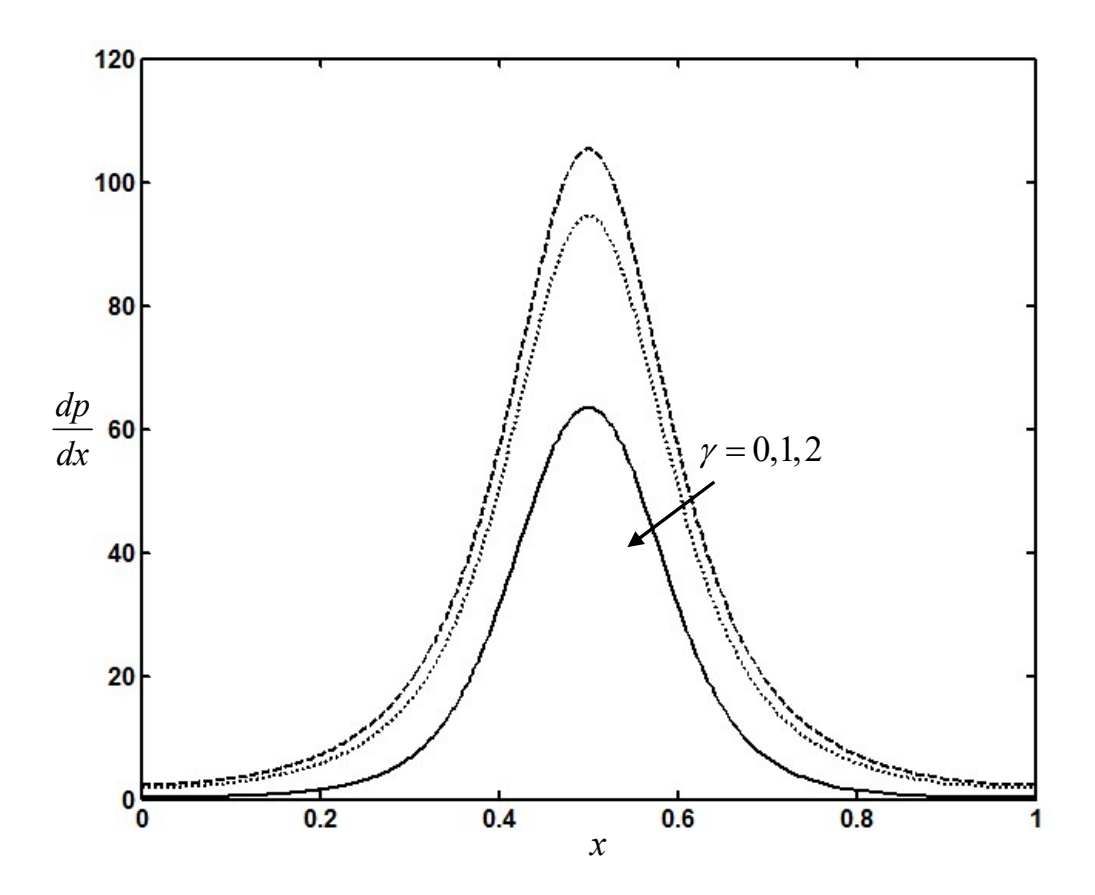


Fig. 3 The variation of the axial pressure gradient $\frac{dp}{dx}$ with γ for e=0.5, Wi=0.02, m=0.3, Da=0.1, M=1, $\phi=0.6$ and $\overline{Q}=-1$.

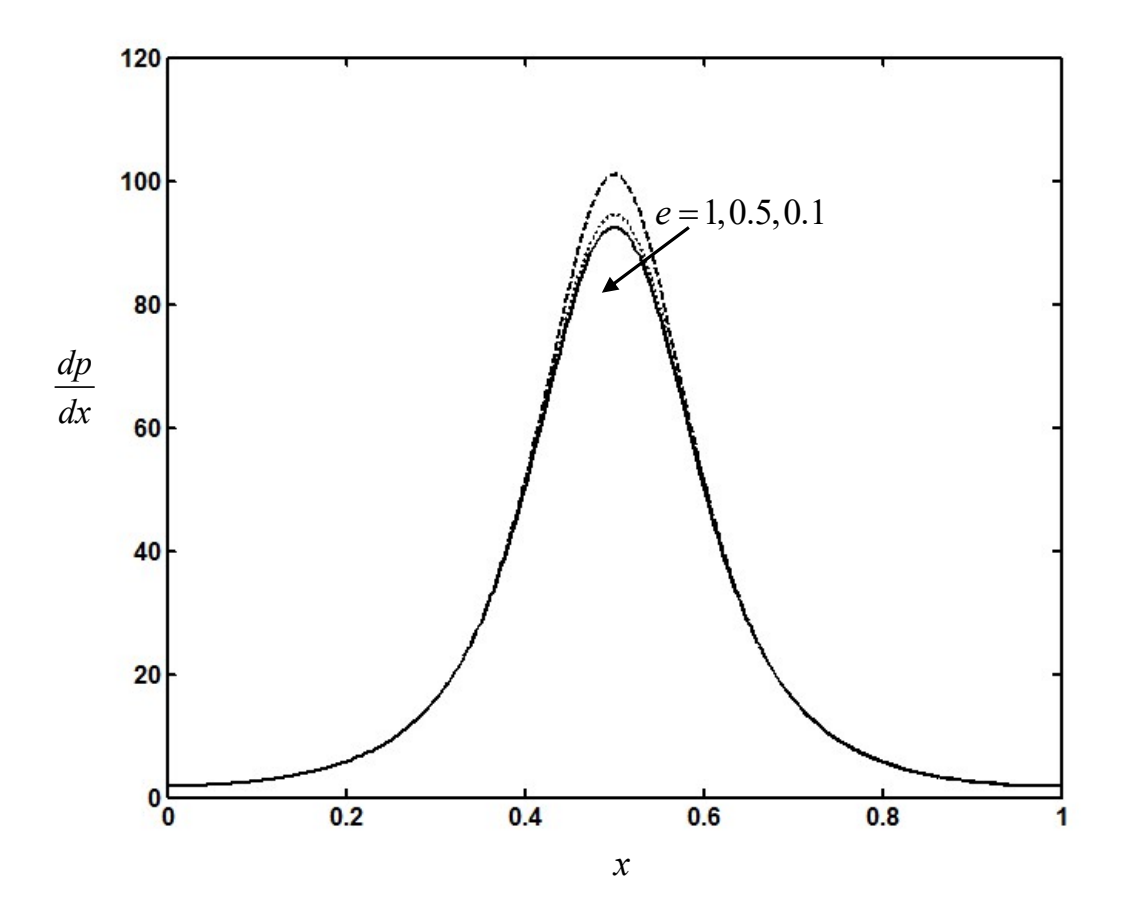


Fig. 4 The variation of the axial pressure gradient $\frac{dp}{dx}$ with e for $\gamma=1$, Wi=0.02, m=0.3, Da=0.1, M=1, $\phi=0.6$ and $\overline{Q}=-1$.

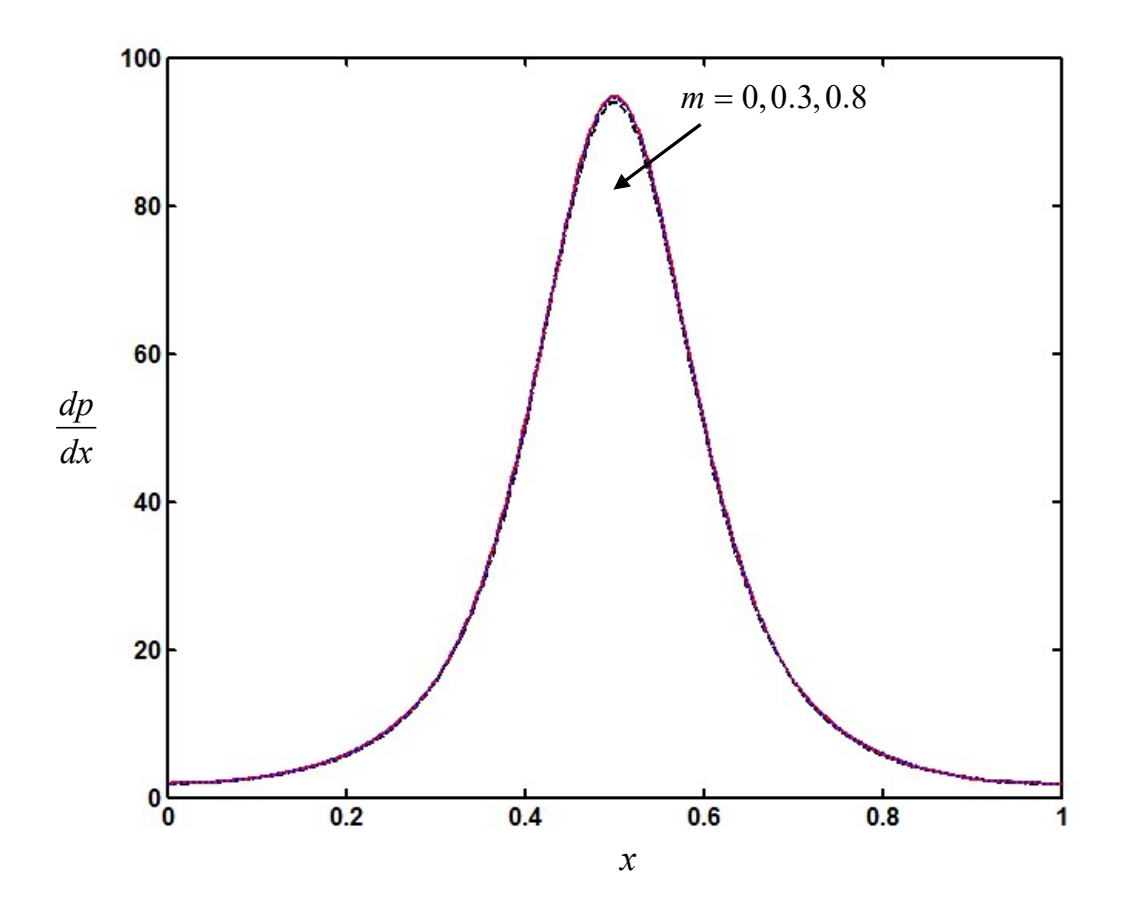


Fig. 5 The variation of the axial pressure gradient $\frac{dp}{dx}$ with m for $\gamma=1$, Wi=0.02, e=0.5, Da=0.1, M=1, $\phi=0.6$ and $\overline{Q}=-1$.

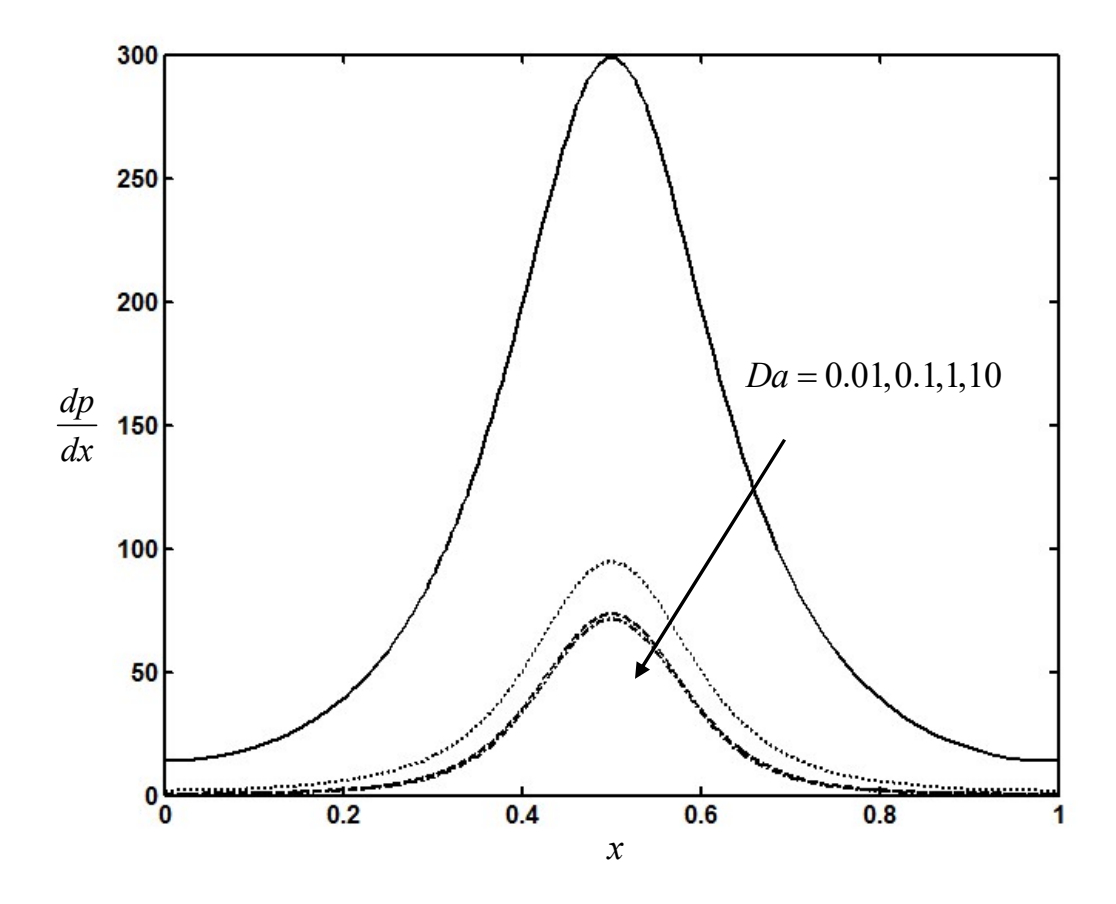


Fig. 6 The variation of the axial pressure gradient $\frac{dp}{dx}$ with Da for $\gamma = 1, Wi = 0.02$, e = 0.5, M = 1, m = 0.3, $\phi = 0.6$ and $\overline{Q} = -1$.

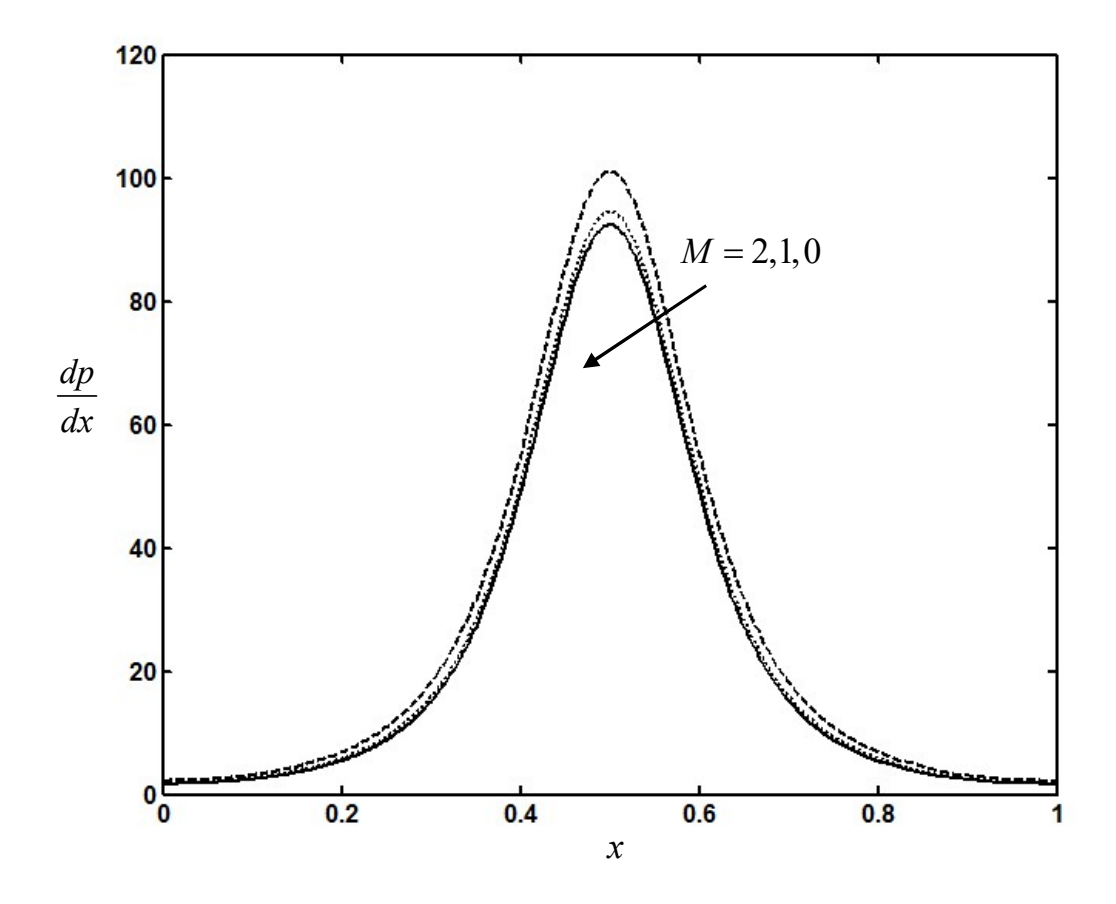


Fig. 7 The variation of the axial pressure gradient $\frac{dp}{dx}$ with M for $\gamma=1$, Wi=0.02, e=0.5, Da=0.1, m=0.3, $\phi=0.6$ and $\overline{Q}=-1$.

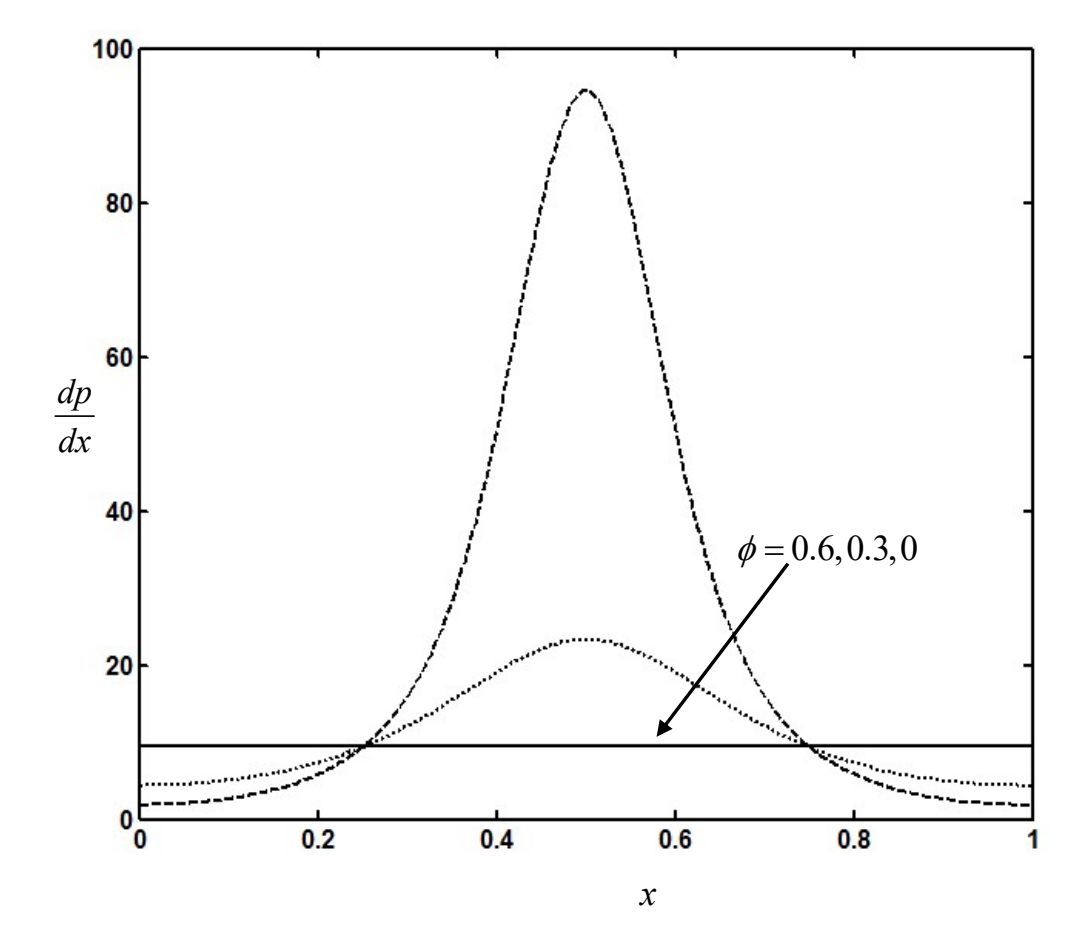


Fig. 8 The variation of the axial pressure gradient $\frac{dp}{dx}$ with ϕ for $\gamma=1$, Wi=0.02, e=0.5, Da=0.1, m=0.3, M=1 and $\overline{Q}=-1$.

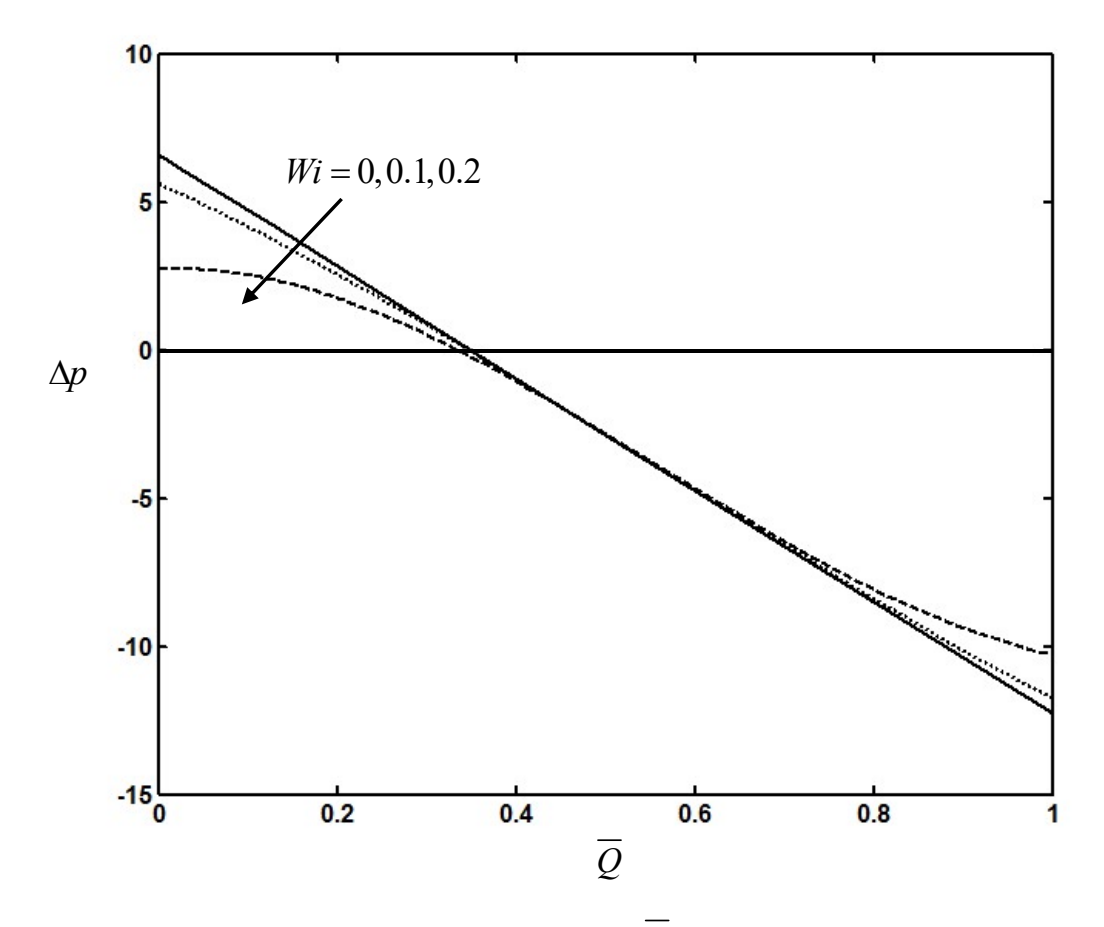


Fig. 9 The variation of the pressure rise Δp with \overline{Q} for different values of Wi with $\gamma = 1$, e = 0.5, Da = 0.1, m = 0.3, M = 1 and $\phi = 0.6$.

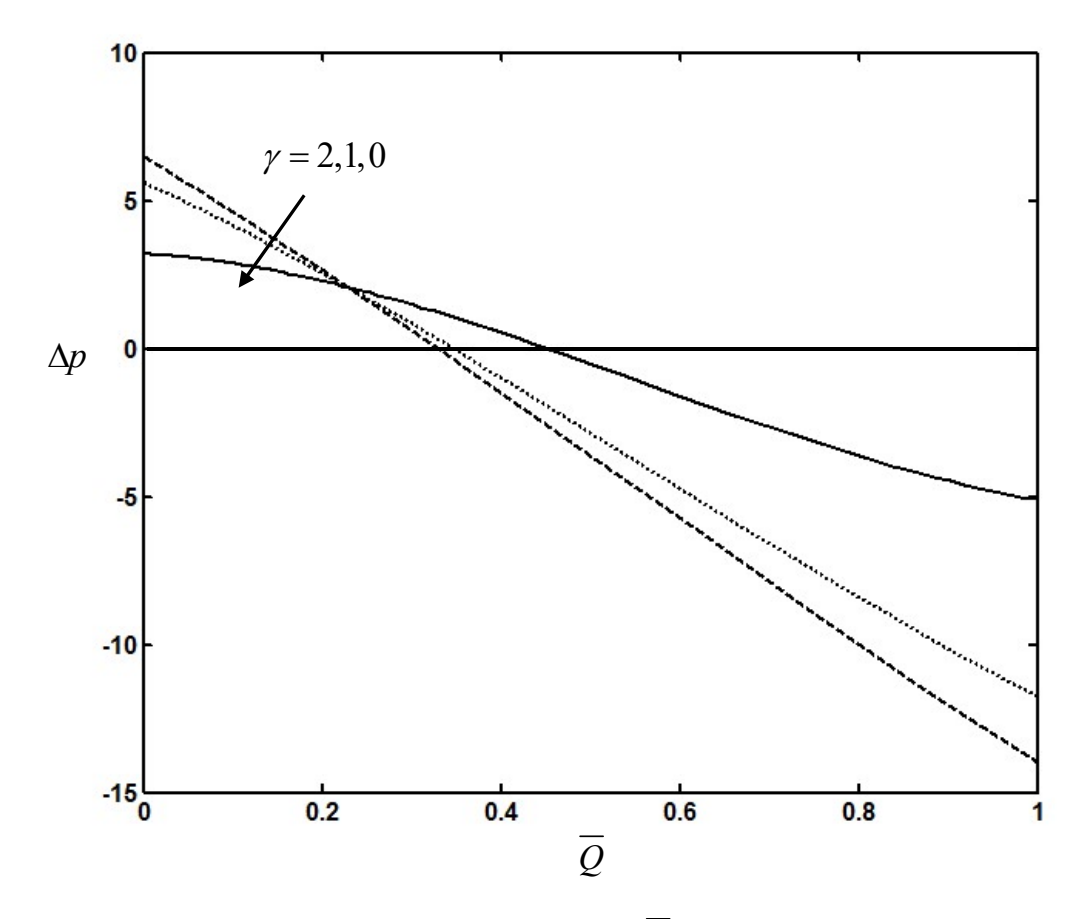


Fig. 10 The variation of the pressure rise Δp with \overline{Q} for different values of γ with e=0.5, Da=0.1, Wi=0.1, m=0.3, M=1 and $\phi=0.6$.

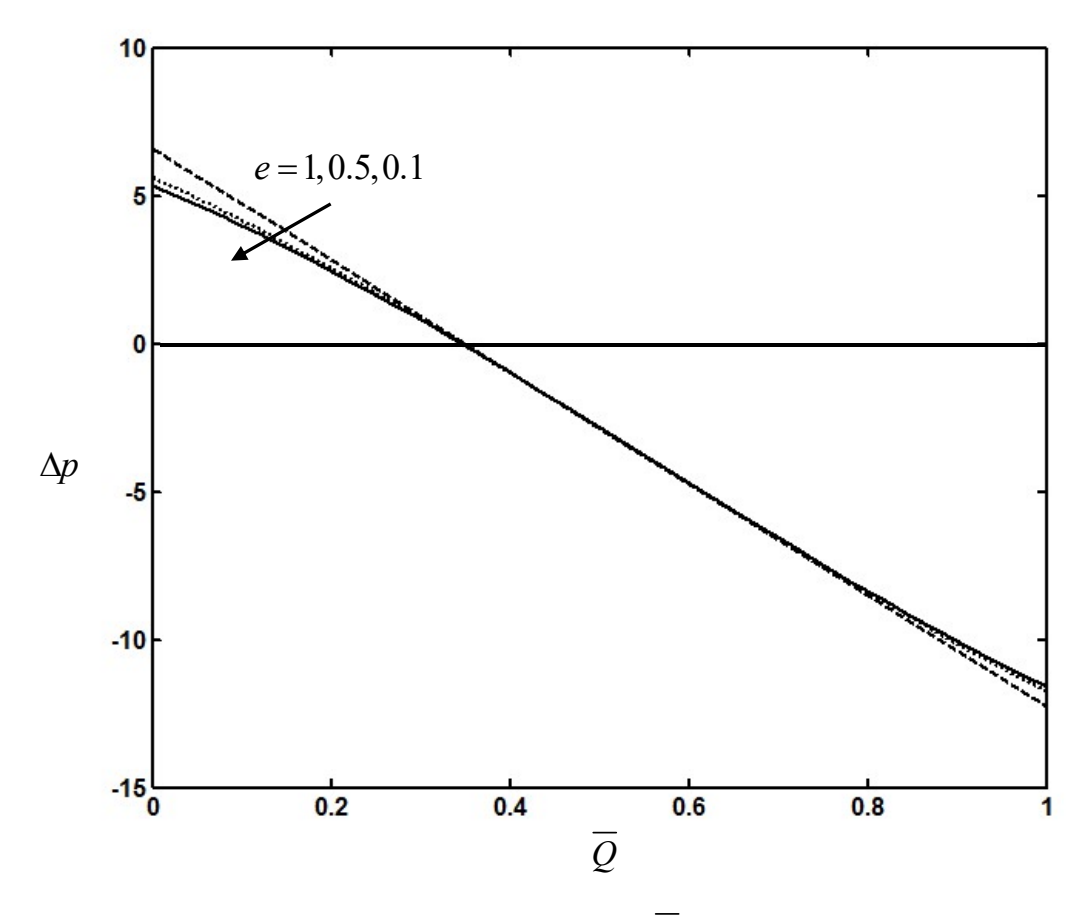


Fig. 11 The variation of the pressure rise Δp with \overline{Q} for different values of e with $\gamma = 1$, Da = 0.1, Wi = 0.1, m = 0.3, M = 1 and $\phi = 0.6$.

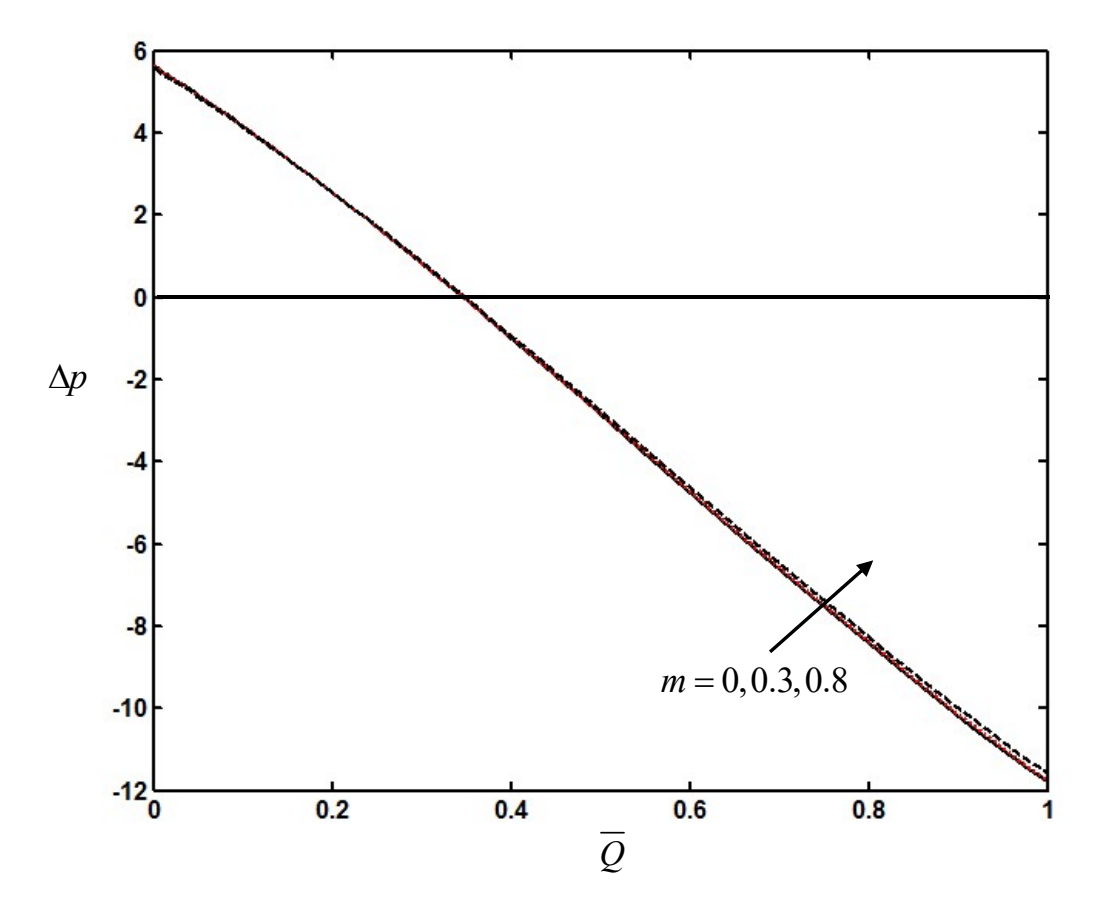


Fig. 12 The variation of the pressure rise Δp with \overline{Q} for different values of m with $\gamma = 1$, Da = 0.1, e = 0.5, Wi = 0.1, M = 1 and $\phi = 0.6$.

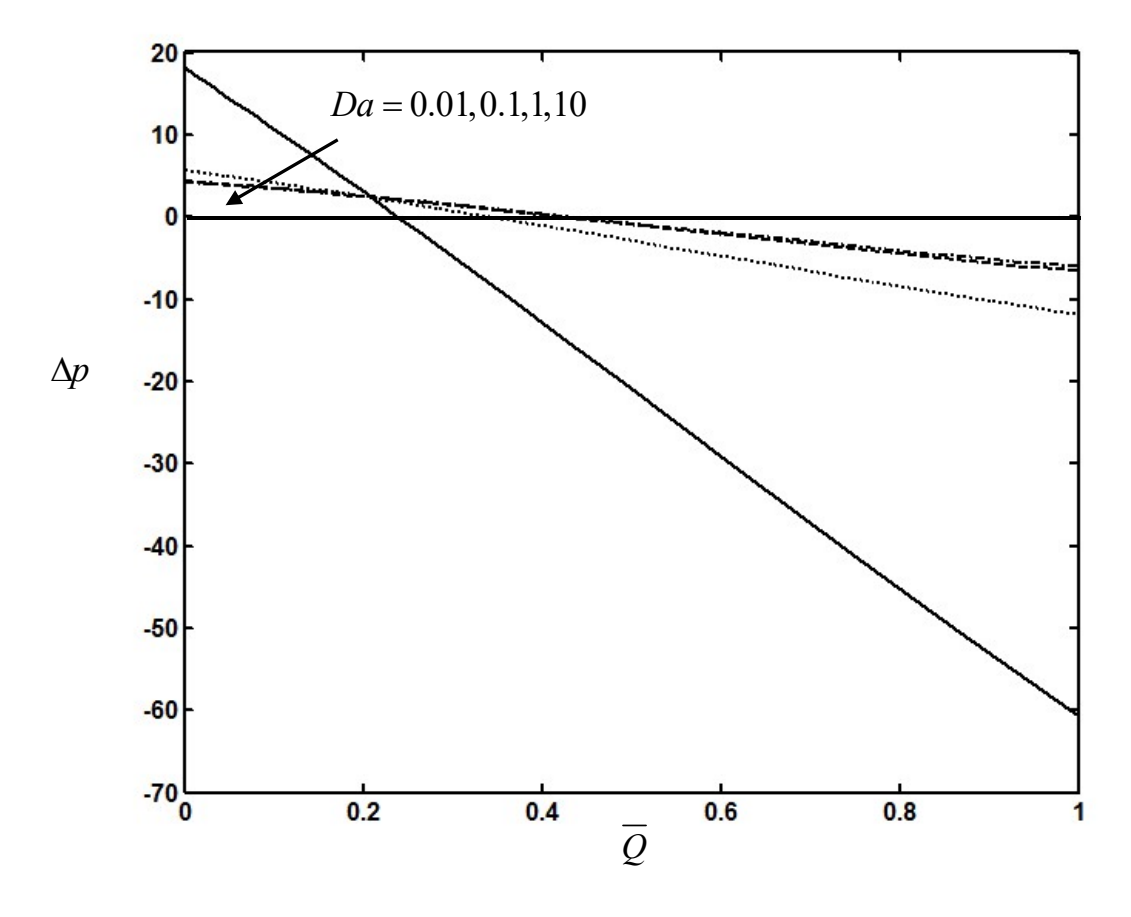


Fig. 13 The variation of the pressure rise Δp with \overline{Q} for different values of Da with $\gamma = 1, M = 1, e = 0.5$, Wi = 0.1, m = 0.3 and $\phi = 0.6$.

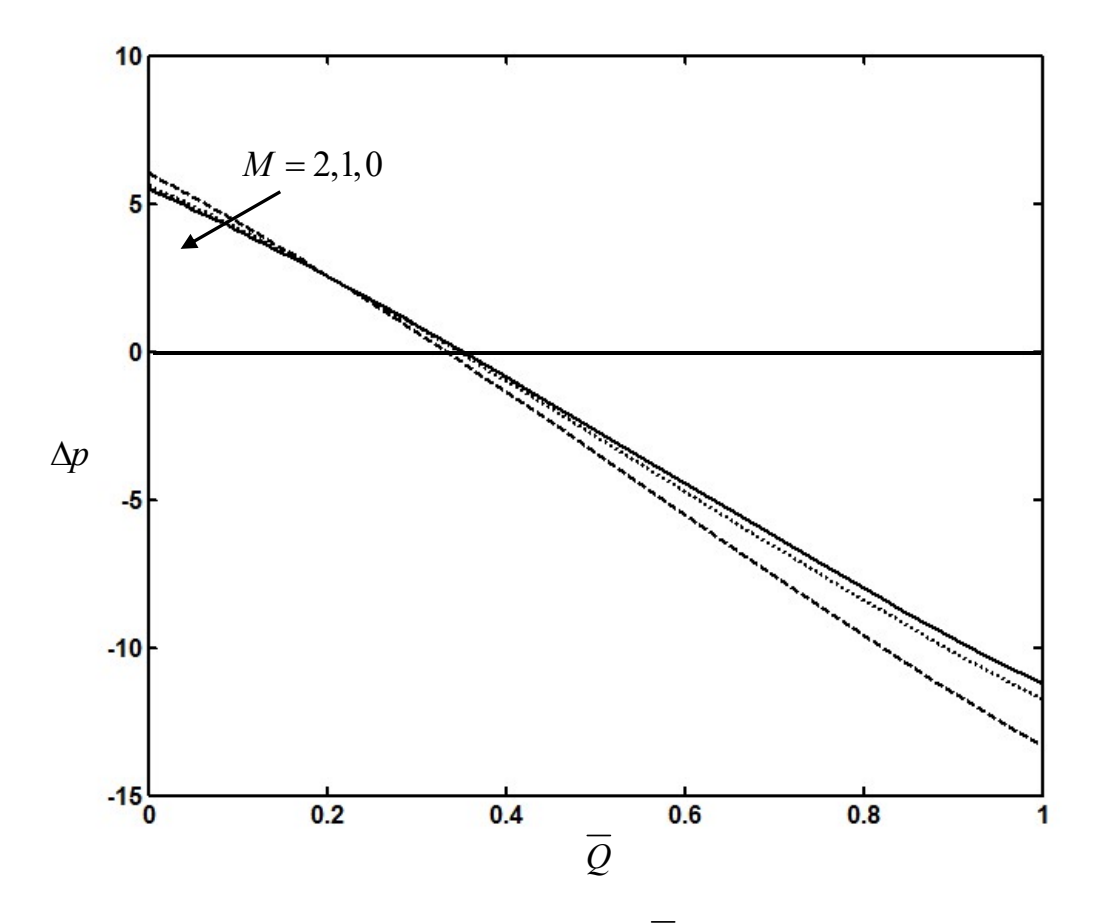


Fig. 14 The variation of the pressure rise Δp with \overline{Q} for different values of M with $\gamma = 1$, Da = 0.1, e = 0.5, Wi = 0.1, m = 0.3 and $\phi = 0.6$.

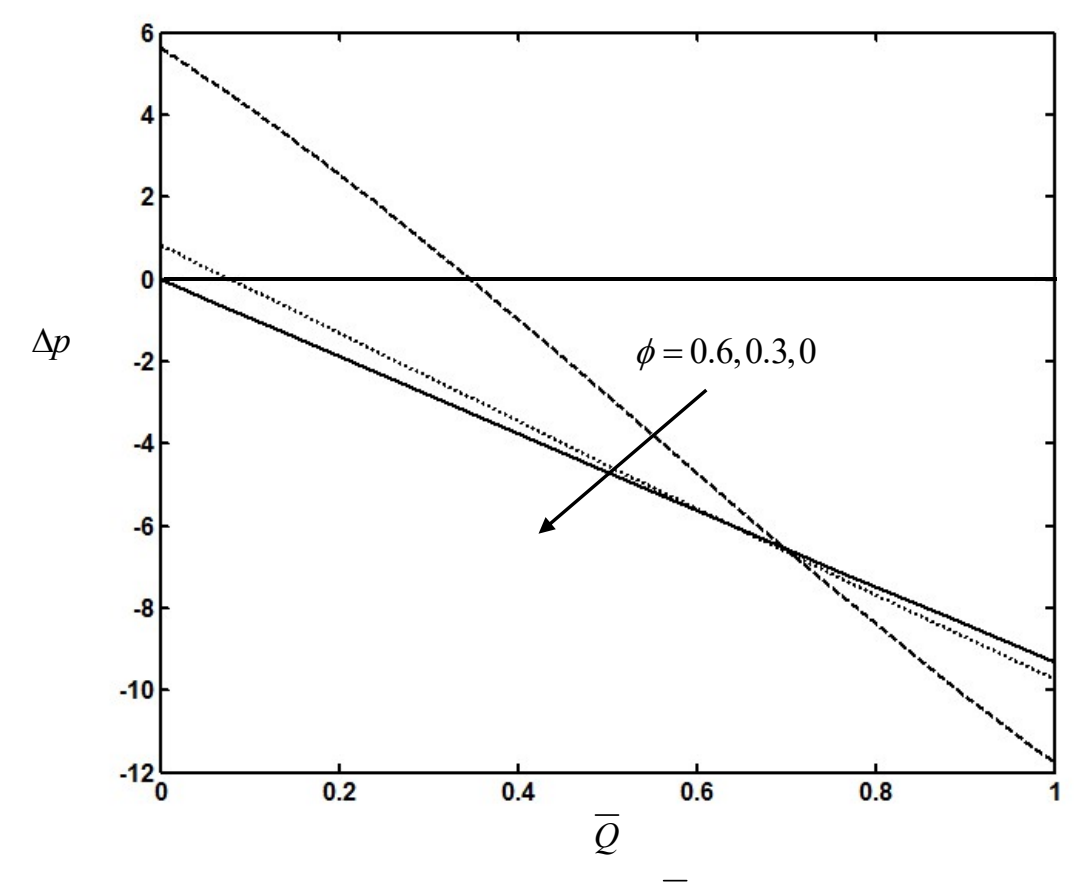


Fig. 15 The variation of the pressure rise Δp with \overline{Q} for different values of ϕ with $\gamma = 1$, Da = 0.1, e = 0.5, Wi = 0.1, m = 0.3 and M = 1

References

Abo-Eldahab, E. M., Barakat, E. I. and Nowar, K. I. Effects of Hall and ion-slip currents on peristaltic transport of a couple stress fluid, International Journal of Applied Mathematics and Physics, 2 (2) (2010), 145–157.

Eldabe, N.T.M., Ahmed Y. Ghaly, A.Y., Sallam, S.N., Elagamy, K. and Younis, Y.M. Hall effect on peristaltic flow of third order fluid in a porous medium with heat and mass transfer, Journal of Applied Mathematics and Physics, 2015, 3, 1138-1150.

Eldabe, N.T., Elogail, M.A., Elshaboury, S.M. and Hasan, A.A. Hall effects on the peristaltic transport of Williamson fluid through a porous medium with heat and mass transfer, Applied Mathematical Modeling, 40(1)(2016), 315-328.

Elshahed, M. and Haroun, M. H. Peristaltic transport of Johnson-Segalman fluid under effect of a magnetic field, Math. Probl. Eng. 6(2005), 663 – 667.

Gad, N.S. Effects of Hall current on peristaltic transport with compliant walls, Appl Math Comput. 235 (2014), 546–554.

Hayat, T. Wang, Y., Siddiqui, A. M. and Hutter K. Peristaltic motion of a Johnson-Segalman fluid in a planar channel, Mathematical Problems in Engineering, 2003 (2003),no. 1, 1-23.

Hayat, T., Ali, N. and Asghar, S. Hall effects on peristaltic flow of a Maxwell fluid in a porous medium, Physics Letters A, 363(5-6) (2007), 397–403.

Johnson JR., M.W. and Segalman, D. A model for viscoelastic fluid behavior which allows nonaffine deformation, J. Non-Newtonian Fluid Mech. 2 (1977), 255–270.

ISSN NO: 1301-2746

Kolkka, R.W., Malkus, D.S., Hansen, M.G., Ieriy, G.R., and Worthing, A.R. Spurt phenomenon of the Johnson–Segalman fluid and related models, J. Non-Newtonian Fluid Mech. 29 (1988), 303–335.

Malkus, D.S., Nohel, J.A., and Plohr, B.J. Dynamics of shear flows of non-Newtonian fluids, J. Comput. Phys. 87 (1990), 464–497.

Mcleish, T.C.B., and Ball, R.C. A molecular approach to the spurt effect in polymer melt flow, J. Polym. Sci. (B) 24 (1986) 1735–1745.

Ranjitha, B. and Subba Reddy, M. V. Radiation Effects on the Peristaltic flow of a Williamson fluid through a porous medium in a planar channel, JUSPS-B Vol. 30(12)(2018), 121-132.

Rao, I. J. and Rajagopal, K. R. Some simple flows of a Johnson-Segalman fluid, Acta Mech. 132(1-4) (1999), , 209–219.

Subba Narasimhudu, K. "Effects of hall on peristaltic flows of conducting fluids", Ph D., Thesis, Rayalaseema University, (2017).